Analysis of Colinear Quasi-Phase-Matching in Nonlinear Photonic Crystals

Alon Bahabad, Noa Voloch, and Ady Arie, *Senior Member, IEEE*

***Abstract*—Standard quasi-phase-matching (QPM) schemes assume exact momentum relations between the interacting beams, thus necessitating the direct use of a reciprocal lattice vector to satisfy momentum balance. Usage of finite width beams for colinear interactions permits to use a projection of the reciprocal lattice vector along the propagation direction of the beams. We analytically derive this result and exam the new options given by this projection-based QPM for the analysis and design of nonlinear optical devices.**

***Index Terms*—Frequency conversion, nonlinear optics, phase-matching.**

I. Introduction

SECOND-order nonlinear optical processes usually suffer from dispersion. As beams of different frequencies propagate at different velocities they become out of phase with each other, thus efficient energy transfer is prevented. This phase mismatch can be formulated in terms of a macroscopic momentum imbalance. However, if the interaction takes place within an engineered nonlinear photonic crystal (NPC), momentum conservation needs to be satisfied only up to a reciprocal lattice vector belonging to the structure [1]. Such a phase-matching is called quasi-phase-matching (QPM) [2], [3]. Usually such processes are analyzed for photons with exact momentum, that is—assuming plane wave interaction [4]–[8]. This might be satisfactory in most cases where structures are designed for maximal interaction efficiency. However, allowing for some uncertainty in the photons momentum by restricting the interaction width can account for interesting phenomena. In particular, it was recently shown, that under such constraints, while interacting within a strictly periodic structure, different processes could acquire quasi-periodic characteristics [9]. In this paper we give a detailed derivation for this new type of QPM for colinear interactions within a periodic structure along with several analysis examples.

Manuscript received December 10, 2007; revised February 6, 2008.

A. Bahabad was with the School of Electrical Engineering, Fleischman Faculty of Engineering, Tel Aviv University, Tel Aviv 69978, Israel. He is now with JILA, University of Colorado, Boulder, CO 80309-0440 USA (e-mail: alonuria@gmail.com).

N. Voloch and A. Arie are with the School of Electrical Engineering, Fleischman Faculty of Engineering, Tel Aviv University, Tel Aviv 69978, Israel (e-mail: noavoloch@gmail.com; ady@eng.tau.ac.il).

Color versions of one or more of the figures in this paper are available online at http://ieeexplore.ieee.org.

Digital Object Identifier 10.1109/JQE.2008.922328

The structure of the paper is as follows: Section II covers the physical background for this work, dealing with QPM under certain conditions leading to the so-called projection-based QPM. Section III demonstrates how the concept of projection-based QPM can be used for the design and analysis of 2-D periodic NPCs for QPM of colinear processes. The main findings are summarized in Section IV. The Appendix gives a rigorous derivation for the spectrum of a projected 2-D periodic lattice, a result which is central to the physical behavior of projection-based QPM.

II. Projection-Based QPM

We start with the evolution equation for second-harmonic-generation (SHG) which is the prototype for any three-wave-mixing process [4]

$$\mathbf{k}_{2\omega}\cdot\nabla E_{2\omega}(\mathbf{r}')=-2i\frac{\omega^2}{c^2}E_{\omega}(\mathbf{r}')^2 d_{ij}(\mathbf{r}')\exp(i\boldsymbol{\Delta}\mathbf{k}\cdot\mathbf{r}'). \quad (1)$$

Here $E_{2\omega}$ is the second-harmonic amplitude generated due to the application of the pump field (with amplitude E_{ω}) upon the nonlinear medium. $\mathbf{k}_{2\omega}$ is its wave vector, ω is the angular frequency of the pump, c is the speed of light in vacuum, and $\boldsymbol{\Delta}\mathbf{k}=\mathbf{k}_{2\omega}-2\mathbf{k}_{\omega}$ is the phase mismatch vector. We assume coupling between the different harmonics through a single, spatially dependent, component $d_{ij}(\mathbf{r}')$ of the nonlinear tensor. The beams are assumed to be paraxial (possessing slowly varying amplitudes). The prime coordinates $\mathbf{r}'=(x',y')$ relate to some general coordinate system in which the structure function $d_{ij}(\mathbf{r}')$ is given.

The role of the phase mismatch is elucidated by integrating the above equation. We do so under the assumption that during the nonlinear frequency conversion process the pump beam would lose only a tiny amount of its power and so we can assume that its power is undepleted (the pump amplitude would be taken as spatially constant). As the type of problems we are interested in are planar in nature, the integration is done over a rectangular area $A=LW$ with length L oriented along the second harmonic wave vector and with width W. The outcome gives the value of the generated second harmonic amplitude at the end of the interaction length [6]

$$E_{2\omega}(\boldsymbol{\Delta}\mathbf{k})=\frac{\kappa}{W}\iint_A d_0(\mathbf{r}')e^{i\boldsymbol{\Delta}\mathbf{k}\cdot\mathbf{r}'}dx'dy' \quad (2)$$

where $\kappa=(-i\omega E_{\omega}^2 d_{ij})/(cn_{2\omega})$ is composed of all the physical constant parameters ($n_{2\omega}$ is the index of refraction for the second harmonic beam). We separated the value of the coupling term into a constant magnitude (d_{ij} within κ) multiplied by a

normalized spatially dependent function: $d_{ij}(\mathbf{r}') = d_{ij}d_0(\mathbf{r}')$. If the phase mismatch is not zero (as is usually the case) and the coupling term is constant—the second harmonic field is proportional to an integration over an oscillating term, which averages out to a negligible value. If, however $d_0(\mathbf{r}')$ contains an oscillating term (in its Fourier expansion) of the same value as (minus) the phase mismatch this oscillation would be cancelled and a significant build up of the radiation would occur, in other words, the process would be phase matched. This occurs when the structure contains spatial correlations, that is, it is ordered. Specifically, if we consider a periodic structure built upon a periodic lattice infrastructure, its Fourier transform (FT) contains a weighted set of distributed Dirac delta functions at locations known as reciprocal lattice vectors (RLV). Each RLV can phase match a nonlinear process whose phase mismatch vector equals the RLV. But this is true under the assumption that the interaction takes place over a very large area compared to the associated wavelengths—that is, for photons with exact momentum. Indeed, this was the regular assumption for the design and analysis of 2-D NPCs [4], [5], [10]. However, allowing (for the realistic) restriction of the interaction width, as exemplified by the use of regular Gaussian beams (or any other finite width beams such as a Bessel beam or a top-hat beam), the photons acquire uncertainty in the transverse direction and phase-matching is possible even if only the longitudinal component of an RLV matches the phase mismatch value. Explicitly we consider colinear processes where all the different harmonic beams propagate in the same direction, resulting in a scalar phase mismatch value in a rotated (by α degrees) coordinate system (x, y) with x oriented along the propagation direction (see Fig. 1). This means that the perpendicular phase mismatch value is nulled: $\Delta k_y = 0$ and we can use a scalar value for the longitudinal component: $\Delta k_x = \Delta k$. If we now define the interaction width as $W = y_1 - y_0$ and set $D(x) = \int_{y_0}^{y_1} dy d(x, y)$ where $d(x, y)$ is a rotated version of $d_0(x', y')$ (with respect to the (x', y') coordinate system), (2) is now given by

$$E_{2\omega}(\Delta k) = \frac{\kappa}{W}\tilde{D}(\Delta k). \tag{3}$$

The spectrum $\tilde{D}(\Delta k)$ is the FT of $D(x)$, which in turn is the projection of the periodic lattice onto the x-axis. Note that the definition of $D(x)$ above is appropriate for a top-hat beam profile, which is not physical. However, provided the interaction is restricted to an area of small diffraction (for example within the Rayleigh range for a Gaussian beam) the top-hat profile can be taken as an acceptable approximation.

We assume the NPC is represented by a distribution of Dirac delta functions convolved with a motif [7]

$$d_0(x', y') = \left[2 \cdot s_0(x', y') \otimes \sum_{m,n} \delta(\mathbf{r}' - m\mathbf{a}_1 - n\mathbf{a}_2)\right] - 1 \tag{4}$$

where $\mathbf{r}' = x'\hat{\mathbf{x}}' + y'\hat{\mathbf{y}}'$, $\otimes$ represents convolution and the lattice primitive vectors are given by $\mathbf{a}_1$ and $\mathbf{a}_2$. The motif is represented geometrically by the function $s_0(x', y')$ which gets the value 1 inside the shape area and 0 otherwise. Note that using the above representation the background is considered to have a value of (-1).

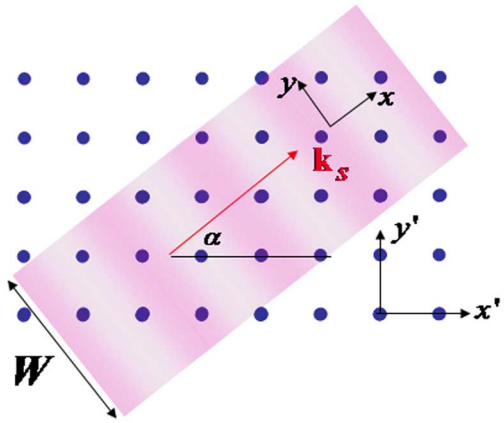

Fig. 1. Geometrical setup for colinear interaction. The NPC is spanned in the (x', y') coordiante system. The interacting beams are aligned with the x direction, belonging to the (x, y) coordinate system.

It can be shown (see the Appendix) that the projected structure function can be written as a Fourier series $D(x) = \sum_{mn} \rho_{mn} \exp(-iK_{mn}x)$. Equivalently the spectrum would be $\tilde{D}(\Delta k) = \sum_{mn} \rho_{mn} \cdot 2\pi\delta(\Delta k - K_{mn})$. Substituting into (3) gives

$$E_{2\omega}(\Delta k) = \frac{\kappa}{W}\sum_{mn} \rho_{mn} \cdot 2\pi\delta(\Delta k - K_{mn}) \tag{5}$$

which explicitly shows that an interaction would be efficient under the phase-matching condition $\Delta k = K_{mn}$ for some (m, n). In that case the amplitude build-up efficiency for the interaction would be proportional to the appropriate Fourier coefficient ρ_{mn}.

We now give expressions for both the spectrum and the Fourier coefficients. For a rigorous derivation one should consult the Appendix. If the reciprocal lattice primitive vectors (conjugate to the primed coordinate system) are $\mathbf{b_1}$ and $\mathbf{b_2}$ then

$$K_{mn} = (mb_{1x'} + nb_{2x'})\cos\alpha + (mb_{1y'} + nb_{2y'})\sin\alpha. \tag{6}$$

In addition

$$\rho_{mn} = 2\frac{W}{V}\mathrm{sinc}\left(\frac{WN(m,n)}{2}\right) \cdot S_0\left(\frac{K_{mn}\cos\alpha - N(m,n)\sin\alpha}{2\pi} \cdot \frac{K_{mn}\sin\alpha + N(m,n)\cos\alpha}{2\pi}\right). \tag{7}$$

Here $N(m, n) = (mb_{1y'} + nb_{2y'})\cos\alpha - (mb_{1x'} + nb_{2x'})\sin\alpha$. S_0 is the FT of the motif area function $s_0(x', y')$. $V = |\mathbf{a}_1 \cdot (\mathbf{a}_2 \times \hat{z})|$ is the real space lattice unit cell area.

The K_{mn} values are just the projection of the set of all reciprocal lattice vectors along the propagation direction x. If the inclination of the propagating beams α with respect to the lattice primitive vectors is irrational the spectrum K_{mn} is characteristic of a quasi-periodic structure [9], [11]. An example for this scenario is given in Section III-C. Note that even though the interaction is analyzed in a scalar manner—along the beams propagation direction, the indexing of the possible phase-matched interaction is 2-D, which is quite obvious given the interaction takes

place within a structure modulated in two dimensions. However, the consequence of this fact is that even if we restrict an interaction to be colinear within a periodic 2-D structure, the wealth of possibilities for phase-matching is the same as for a colinear interaction within a structure with a quasi-periodic 1-D modulation.

What happens if we revert back to a plane-wave (exact momentum) approximation? In this case in which $W \rightarrow \infty$, we get $W\mathrm{sinc}(WN(m,n)/2) \rightarrow \pi\delta(N(m,n))$. This means that there would be a nonvanishing Fourier coefficient only for $N(m,n) = 0$ which gives $\tan(\alpha) = (mb_{1y'} + nb_{2y'})/(mb_{1x'} + nb_{2x'}) = \tan[\angle(m\mathbf{b_1} + n\mathbf{b_2})]$, which together with (6) gives $K_{mn} = m\mathbf{b_1} + n\mathbf{b_2}$. That is—for plane waves, phase-matching occurs only when the phase mismatch vector exactly equals a reciprocal lattice vector, which is the standard phase-matching condition [4], [7]. The Fourier coefficient in this case would be $(1/V)S_0(K_{mn}/2\pi)$.

The above results can be modified for a 1-D NPC represented by $d_0(x') = [2 \cdot s_0(x') \otimes \sum_m \delta(x' - ma)] - 1$, which is a set of repeated motifs spaced with length a apart. Now there would be only one reciprocal lattice base vector $b = 2\pi/a$ and the location of the Dirac delta functions in K-space would be in $K_m = mb\cos\alpha$. In addition $N \rightarrow N(m) = -mb\sin\alpha$, $V \rightarrow a$ and S is sampled with a single reciprocal coordinate. This all means that the related coefficients would be $\rho_m = (W/a)\mathrm{sinc}(WN(m)/2) \cdot 2S(K_m/2\pi)$.

III. Analysis of Colinear Interactions

The expressions given above can also serve as an analysis tool for colinear interactions. We examine a few cases.

A. Typical Colinear Second-Harmonic Response

We begin with a simulation of the second-harmonic response of a hexagonal NPC. We use a design which is characteristic of NPCs for near infrared fundamental radiation. The simulated material is Stoichiometric Lithium Tantalite. The primitive vectors of the lattice are 12.6 μm$\angle 0^\circ$ and 12.6 μm$\angle 120^\circ$. A circular motif of diameter 5.1 μm representing a positive nonlinear material polarization $+\chi^{(2)}$ is attached to every lattice point. The background is assumed to be of negative value $-\chi^{(2)}$. In this simulation all possible colinear SHG for wavelength of 1047.5 nm as a function of propagation direction and temperature are shown at a normalized efficiency scale in Fig. 2. The interaction width was restricted to 5 μm. Brighter color corresponds to a better efficiency. For a finite interaction length of L the efficiency is proportional to $|\rho_{mn}\mathrm{sinc}[(L/2)(\Delta k - M_{mn})]|^2$ with the sinc term accounting for imperfect phase-matching conditions. Each parabola represent colinear phase-matching by a given reciprocal lattice vector (whose m, n indices are indicated). The apex of each parabola corresponds to phase-matching using the whole reciprocal lattice vector, the situation which is applicable to "real" plane wave interaction. The other parabola points corresponds to projection-based phased matching, existing only when the interaction width is restricted. We see that there are much more options for projection-based QPM than for standard QPM, albeit at the price of efficiency.

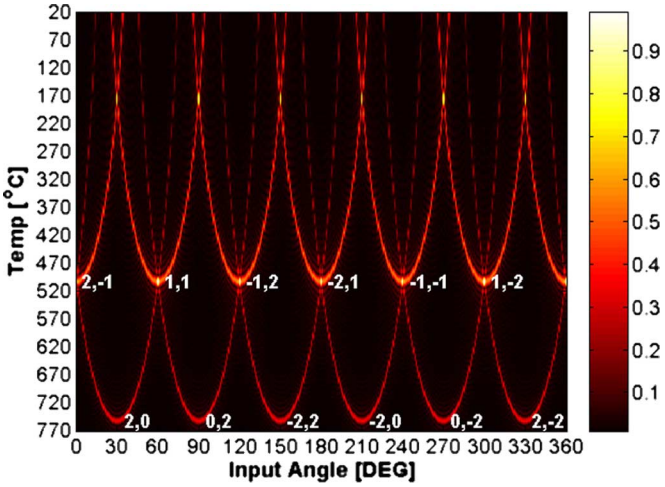

Fig. 2. Second-harmonic response of a hexagonal NPC. Simulated normalized efficiency of colinear SHG as a function of temperature and angle of propagation for a restricted-width interaction. Each parabola corresponds to the contribution of a single reciprocal lattice vector whose indices are indicated near the apex of the parabola.

From (5) and (7) we note that the dependency on the interaction width W is a simple sinc function. Reducing the interaction width reduces the variation in efficiency along each parabola such that the efficiency of projection-based QPM is closer to that of standard QPM. For an experimental demonstration of projection-based QPM and related efficiencies the reader is kindly referred to our previous work [9].

B. Possibilities for Phase Matching

We can consider questions regarding the possibility of a certain process. Unlike with standard (plane waves interaction) QPM where such questions are easily addressed using a cosines law [4] here the geometry involves projection of all the reciprocal lattice vectors which makes things a little more complicated. However, using simple results from the geometry of numbers several possibility questions can be formulated and solved. We start with the following: given a specific NPC and a specific propagation direction (defined by α) within the NPC, which processes can be phase matched? To solve the problem let us define the phase-matching condition (6) in an alternative way

$$\Delta k = \Delta k_{mn} = nk^{(1)}(\alpha) + mk^{(2)}(\alpha) \tag{8}$$

where we know that m and n are integers. But if we treat m and n as real numbers we can define a line equation (denoted as l) in the (m,n) plane

$$l : n = -\frac{k^{(2)}}{k^{(1)}}m + \frac{\Delta k}{k^{(1)}}. \tag{9}$$

The question whether a process with a specific Δk can be phase matched is now given in the form of finding whether for this Δk the line equation l has integer solution for m and n. Put otherwise, the question is—whether the line l intersects the fundamental lattice in the (m,n) plane (the fundamental lattice is the

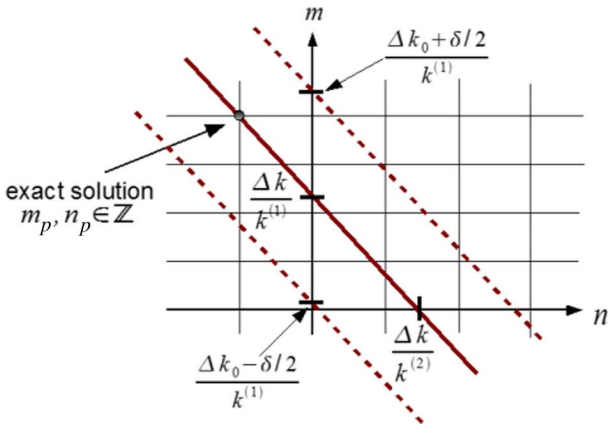

Fig. 3. Finding whether a specific processes at a specific propagation direction can be phase matched is equivalent to finding intersections of a line with the fundamental lattice, while tolerant phase-matching is equivalent to finding points of the fundamental lattice within a strip area.

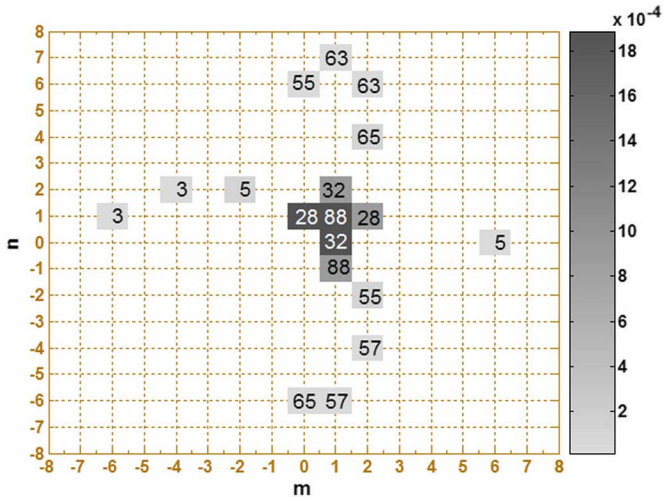

Fig. 4. Simulation of the feasibility for two tolerant colinear SHG processes taking place within the hexagonal NPC. A square denotes a solution at a specific (m,n) value. The number inside the square is the corresponding angle of propagation α in degrees and its color corresponds to the absolute value of the accompanying Fourier coefficient.

set of all points with integer coordinates). An example in which a solution exists is depicted in Fig. 3.

To find the answer to the equivalent geometrical question we do the following: the numerator and denominator of each of the line parameters are multiplied by a common integer

$$l: n = -\frac{k^{(2)} \cdot a}{k^{(1)} \cdot a} m + \frac{\Delta k \cdot b}{k^{(1)} \cdot b} \tag{10}$$

such that they are now relatively prime, that is they have no common divisor except for 1. In other words, their greatest common divisor (gcd) is 1 $\gcd(k^{(2)} \cdot a, k^{(1)} \cdot a) = \gcd(\Delta k \cdot b, k^{(1)} \cdot b) = 1$. Then, a solution exists if b divides a [13], that is, if we can write $a = bp$ where p is some other integer. A natural conclusion is that a specific process in a specific propagation direction is not always feasible.

However, we can mitigate the condition for exact phase-matching by introducing some tolerance: let us denote the condition for exact phase-matching as Δk_0 and let us now consider as acceptable every process with phase-matching which obeys $|\Delta k - \Delta k_0| \leq \delta$ where δ is the tolerance. The equivalent geometric question is whether the strip area depicted in Fig. 3 contains any points of the fundamental lattice. In this case a solution exists if $\delta > 1/a$ [13].

As an example consider a simulation of two second harmonic generation processes at pump wavelengths of 1047.5 and 1550 nm taking place within the hexagonal NPC as depicted in Fig. 4. The operating temperature was set to 23° while the tolerance was chosen to be 2500 [1/m]. In this figure each square represents a tolerant solution at the angle written within it while its coordinates are the phase-matching order (m,n). Its color represents the accompanying Fourier coefficient for exact phase-matching condition [(7)]. Note that the solutions come in pairs (for each angle we have two processes). The best solutions are given for propagation angles of 32° and 88°. Reducing the tolerance reduces the number of possible solutions.

Another question we can consider is the following. Given a specific process (defined by a specific Δk) find which order can give a solution in which angle? To solve this problem let us define again the phase-matching condition (6) in yet another way

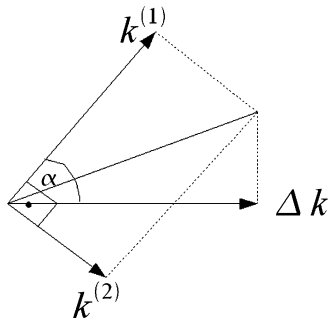

Fig. 5. Condition for phase-matching a process at a specific (m,n) order and a specific angle α.

$$\Delta k = k^{(1)}(m,n)\cos\alpha + k^{(2)}(m,n)\sin\alpha. \tag{11}$$

A geometric representation of a solution is very illustrative as can be seen in Fig. 5: drawing the newly defined vectors $k^{(1)}$ and $k^{(2)}$ as an orthogonal basis we can see that the solution Δk is equal to the projection of the diagonal of the rectangle whose edges are the basis vectors. The conclusion is that we can always find a solution. All we should do is choose $k^{(1)}$ and $k^{(2)}$ long enough (by taking appropriate values of m and n) so that the above diagonal would be equal or bigger than Δk: $(\Delta k)^2 \leq \left(k^{(1)}\right)^2 + \left(k^{(2)}\right)^2$ and then turn the rectangle around until we find the appropriate angle α in which the diagonal projection is equal to the phase mismatch value.

C. Quasiperiodicity in a Periodic Lattice

As was noted earlier, when the inclination of the propagating beams with respect to the lattice primitive vectors is irrational the spectrum K_{mn} is characteristic of a quasi-periodic structure. To illustrate the emergence of quasi-periodic characteristics we

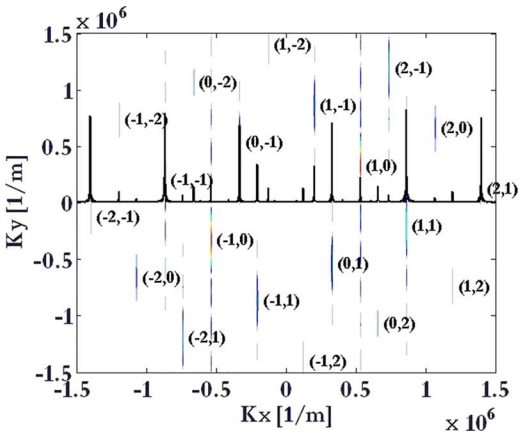

Fig. 6. Fibonacci-type spectrum given by projection of a square lattice NPC. Warmer colors correspond to stronger peak values. The relevant values for the projection-based QPM are obtained for $k_y = 0$ (indicated by the black line) which is the colinear condition in reciprocal space.

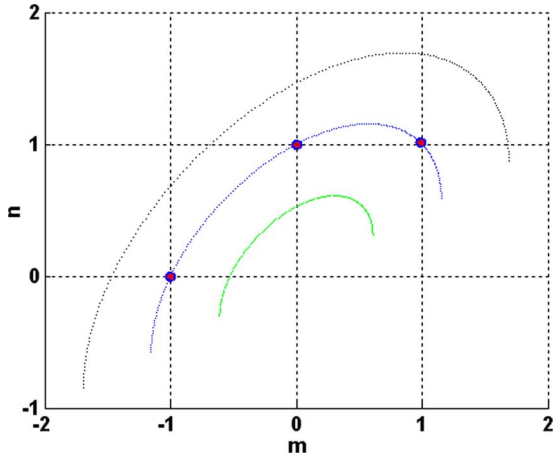

Fig. 7. Solving for plane waves interacting within the hexagonal NPC at 100° centigrades. Each curve corresponds to a different fundamental wavelength (and hence a different Δk). The curves are parametrically dependent on the angle of propagation α. The gray (outer) curve is for fundamental wavelength of 1047.5 nm, the blue (middle) is for 1192.8 nm and the green (inner) is for 1550 nm. The blue (middle) curve has three integer (m, n) solutions corresponding to three different propagation directions in which colinear phase-matching is possible.

consider an NPC based on a square lattice. If the interacting beams are propagating at an angle α to one of the principle axes such that $\tan(\alpha) = 1/\tau$, where $\tau = (1+\sqrt{5})/2$ is the golden ratio, the available phase-matching values [(6)] are ordered according to the spectrum of the famous quasi-periodic Fibonacci tiling [14]. Specifically for a square lattice with edges of unit length the spectrum is located at $K_{mn} = 2\pi(m\tau+n)/\sqrt{\tau+2}$. The occurrence of such a spectrum through the projection of a square lattice with edges of 10 μm and a circular repeated motif of radius 2 μm is shown in Fig. 6. These dimensions are representatives for actual NPCs and they entail a 10^5 scaling factor for the spectrum mentioned above. The figure contains the FT of the structure restricted by an interaction width of 20 μm. The different peaks of the spectrum are enumerated by their location in reciprocal space in values of reciprocal lattice vectors. The finite interaction width results in a smearing of the peaks. The projection operation manifested by the colinear interaction of the beams results in the spectrum along the line $k_y = 0$. This specific spectrum is superimposed as a 1-D graph (black line) at the middle of the figure.

D. Plane-Waves Solution

Finally we would like to degenerate the general analysis back to the case of plane waves. In the previous section we saw that for plane waves $(W \to \infty)$ nonvanishing values for the Fourier coefficients would be given only if $N_{mn} = 0$. Then a specific processes is phase matched if in addition $\Delta k = (mb_{1x'} + nb_{2x'})\cos\alpha + (mb_{1y'} + nb_{2y'})$ which can also be written in short form as $\Delta k = M_{mn}$. Here we have two equations in m, n and α, which can be solved parametrically in the following way: we first treat m and n as real numbers. Then—for each α we solve the above equations. Running through a range of angles (typically $[0-\pi]$) we draw a parametric curve in the (m, n) plane. If this curve intersect the fundamental lattice we have found a valid solution for plane waves interacting colinearly. An example is illustrated in Fig. 7 for the hexagonal NPC.

IV. Summary

We have developed a formalism for calculating the efficiency of a second-order nonlinear optical process, when the interaction is colinear, width-restricted and takes place within a periodic (1-D or 2-D) NPC. In this case it was shown that the set of phase-mismatch values that can be compensated are equal to the projection of all the reciprocal lattice vectors along the beams propagation direction. An exact expression was given for calculating the resulting field amplitude under the nondepletion approximation. Several analysis examples using this formalism were given, including: finding the conditions for projection phase-matching, as well as a procedure for determining the phase-matching order and angle. As the beam width is increased, the efficiency of the projection phase-matching process diminishes, and in the plane-wave, infinite-beam-width limit, phase-matching occurs only if the phase mismatch vector exactly equals a reciprocal lattice vector. This predicted projection-based QPM together with its ability to give rise to quasi-periodic characteristics were verified experimentally [9].

Appendix
Deriving the Spectrum of a 2-D Periodic Lattice Projected Onto a Line

The spectrum for the projection of a square lattice onto a line was given in a work by Zia and Dallas [11]. Here we treat the most general periodic case—that is—projection of any NPC built upon a periodic 2-D lattice.

The function that represents the projection of the lattice points inside the strip is

$$D(x) = \int dy \cdot r(y) \cdot d(x, y) \tag{12}$$

where $d(x, y) = d_0(x\cos\alpha - y\sin\alpha, x\sin\alpha + y\cos\alpha)$ is a rotated version of $d_0(x', y')$ and $r(y) = \begin{cases} 1, & |y| < W/2 \\ 0, & else \end{cases}$ is the strip-window function. The integration limits for this and

for all subsequent integrals are from $-\infty$ to $+\infty$. We look for the 1-D FT of (12) in the variable x

$$F(u) = \mathrm{FT}_{1Dx}\{D(x)\} \tag{13}$$

where FT_{1Dx} should be read as—the 1-D FT related to the variable x. We use the fact that if $G(u) = \mathrm{FT}_{1D}\{g(x)\}$ then $G(0) = \int g(x)dx$ to describe (12) using a FT

$$D(x) = \mathrm{FT}_{1Dy}\{r(y)\cdot d(x,y)\}\,|_{v=0} \tag{14}$$

where v is the spatial frequency related to y (as u is to x). We can write the last equation as

$$D(x) = \mathrm{FT}_{1Dy}\{r(y)\}\,|_{v=0} \otimes \mathrm{FT}_{1Dy}\{d(x,y)\}\,|_{v=0}. \tag{15}$$

Using $R(v) = \mathrm{FT}_{1Dy}\{r(y)\}$ and $M(x,v) = \mathrm{FT}_{1Dy}\{d(x,y)\}$ we can write the last result as

$$\begin{aligned} D(x) &= R(v)|_{v=0} \otimes M(x,v)|_{v=0} \\ &= \int M(x,\tau)R(v-\tau)d\tau|_{v=0} \\ &= \int M(x,\tau)R(-\tau)d\tau. \end{aligned} \tag{16}$$

Substituting the last result back into (13) we get

$$\begin{aligned} F(u) &= \int d\tau R(-\tau)\mathrm{FT}_{1Dx}\{M(x,\tau)\} \\ &= \int d\tau R(-\tau)L(u,\tau) = \int dv R(-v)L(u,v) \end{aligned} \tag{17}$$

where in the last stage we used $L(u,\tau) = \mathrm{FT}_{1Dx}\{M(x,\tau)\}$ and a change of variables $\tau \rightarrow v$. In fact we can now understand that $L(u,v) = \mathrm{FT}_{2D}\{d(x,y)\}$. Because the FT retains rotation $L(u,v)$ is a rotated version of $L_0(f_{x'},f_{y'}) = \mathrm{FT}_{2D}\{d_0(x',y')\}$, that is

$$L(u,v) = L_0(u\cos\alpha - v\sin\alpha, u\sin\alpha + v\cos\alpha). \tag{18}$$

Using (4)

$$\begin{aligned} &L_0(f_{x'},f_{y'}) \\ &= \mathrm{FT}_{2D}\left\{\left[2\cdot s_0(x',y') \otimes \sum_{m,n}\delta(\mathbf{r}'-m\mathbf{a}_1-n\mathbf{a}_2)\right]-1\right\} \\ &= 2\cdot \mathrm{FT}_{2D}\{s_0(x',y')\}\cdot \mathrm{FT}_{2D}\left\{\sum_{m,n}\delta(\mathbf{r}'-m\mathbf{a}_1-n\mathbf{a}_2)\right\} \\ &\quad - \delta(f_{x'},f_{y'}) \\ &= 2\cdot S_0(f_{x'},f_{y'})\cdot Y_0(f_{x'},f_{y'}) - \delta(f_{x'},f_{y'}). \end{aligned} \tag{19}$$

A well-known crystallographic result gives [12]

$$\begin{aligned} Y_0(f_{x'},f_{y'}) &= \mathrm{FT}_{2D}\left\{\sum_{m,n}\delta(\mathbf{r}'-m\mathbf{a}_1-n\mathbf{a}_2)\right\} \\ &= \frac{1}{V}\sum_{m,n}\delta\left[\mathbf{f}-\frac{1}{2\pi}(m\mathbf{b}_1+n\mathbf{b}_2)\right] \\ &= \frac{1}{V}\sum_{m,n}\delta\left[f_{x'}-\frac{1}{2\pi}(mb_{1x'}+nb_{2x'})\right] \\ &\quad \cdot\delta\left[f_{y'}-\frac{1}{2\pi}(mb_{1y'}+nb_{2y'})\right] \end{aligned} \tag{20}$$

where $\mathbf{b_1}$ and $\mathbf{b_2}$ are the reciprocal lattice basis vectors

$$\begin{aligned} \mathbf{b}_1 &= 2\pi\frac{\mathbf{a}_2\times\hat{z}'}{\mathbf{a}_1\cdot(\mathbf{a}_2\times\hat{z}')} \\ &= \frac{2\pi}{a_{1x'}a_{2y'}-a_{1y'}a_{2x'}}[a_{2y'}\hat{x}'-a_{2x'}\hat{y}'] \\ \mathbf{b}_2 &= 2\pi\frac{\hat{z}'\times\mathbf{a}_1}{\mathbf{a}_1\cdot(\mathbf{a}_2\times\hat{z}')} \\ &= \frac{2\pi}{a_{1x'}a_{2y'}-a_{1y'}a_{2x'}}[-a_{1y'}\hat{x}'+a_{1x'}\hat{y}'] \end{aligned} \tag{21}$$

and $V = |\mathbf{a}_1\cdot(\mathbf{a}_2\times\hat{z})| = |a_{1x}a_{2y}-a_{1y}a_{2x}|$ is the real space (direct) lattice unit cell area. Letting Y be the rotated version of Y_0 and reverting to angular spatial frequencies ($k = 2\pi u, p = 2\pi v$) we get

$$\begin{aligned} Y(k,p) = \frac{4\pi^2}{V}\cdot\sum_{m,n}&\delta[k-(mb_{1x'}+nb_{2x'})\cos\alpha \\ &-(mb_{1y'}+nb_{2y'})\sin\alpha] \\ \cdot\,&\delta[p-(mb_{1y'}+nb_{2y'})\cos\alpha \\ &+(mb_{1x'}+nb_{2x'})\sin\alpha]. \end{aligned} \tag{22}$$

Using the following short-hand notation: $M(m,n) = (mb_{1x'}+nb_{2x'})\cos\alpha + (mb_{1y'}+nb_{2y'})\sin\alpha$, $N(m,n) = (mb_{1y'}+nb_{2y'})\cos\alpha - (mb_{1x'}+nb_{2x'})\sin\alpha$ and using the presentation $k = 2\pi u$ we can write

$$Y(u,p) = \frac{2\pi}{V}\sum_{m,n}\delta\left[u-\frac{M(m,n)}{2\pi}\right]\cdot\delta[p-N(m,n)]. \tag{23}$$

Returning back to (17) while using angular spatial frequencies, we get

$$F(u) = \frac{1}{2\pi}\int dp R(-p)L(u,p). \tag{24}$$

We also note that (18) can be written as

$$L(u,p) = 2\cdot S\left(u,\frac{p}{2\pi}\right)\cdot Y(u,p) - 2\pi\delta(u,p) \tag{25}$$

with S being a rotated version of S_0 (in α degrees). In addition it is quite trivial that $R(p) = W\mathrm{sinc}(pW/2)$ where $\mathrm{sinc}(x) =$

$\sin(x)/x$. Together with a substitution of (23) and (25) in (24), we get

$$\begin{aligned} F(u) &= \left(\frac{1}{2\pi}\right)\int dpW\mathrm{sinc}\left(\frac{pW}{2}\right) \\ &\quad\cdot\left[\frac{2\pi}{V}\sum_{m,n}\delta\left[u-\frac{M(m,n)}{2\pi}\right]\cdot\delta\left[p-N(m,n)\right]\right] \\ &\quad\cdot 2S\left(u,\frac{p}{2\pi}\right)-\delta(u,p)\int dpW\mathrm{sinc}\left(\frac{pW}{2}\right) \\ &= \left[\frac{1}{V}\sum_{m,n}W\mathrm{sinc}\left(\frac{WN(m,n)}{2}\right)\delta\left[u-\frac{M(m,n)}{2\pi}\right]\right] \\ &\quad\cdot 2S\left(u,\frac{N(m,n)}{2\pi}\right)-W\delta(u) \\ &= \left[\frac{W}{V}\sum_{m,n}\mathrm{sinc}\left(\frac{WN(m,n)}{2}\right)\cdot 2\pi\delta\left[k-M(m,n)\right]\right] \\ &\quad\cdot 2S\left(\frac{k}{2\pi},\frac{N(m,n)}{2\pi}\right)-2\pi W\delta(k). \end{aligned} \tag{26}$$

This result gives us a weighted distribution of Dirac delta functions located in K-space at the following locations:

$$\begin{aligned} K_{mn} &= M(m,n) \\ &= (mb_{1x'}+nb_{2x'})\cos\alpha+(mb_{1y'}+nb_{2y'})\sin\alpha. \end{aligned} \tag{27}$$

Ignoring the zero spatial frequency component $\delta(k)$ and inverse FT (26), we get

$$D(x)=\sum_{mn}\rho_{mn}\exp(-iK_{mn}x) \tag{28}$$

where the Fourier coefficients are

$$\begin{aligned} \rho_{mn} &= \frac{W}{V}\mathrm{sinc}\left(\frac{WN(m,n)}{2}\right)\cdot 2S\left(\frac{K_{mn}}{2\pi},\frac{N(m,n)}{2\pi}\right) \\ &= 2\frac{W}{V}\mathrm{sinc}\left(\frac{WN(m,n)}{2}\right) \\ &\quad\cdot S_0\left(\frac{K_{mn}\cos\alpha-N(m,n)\sin\alpha}{2\pi},\right. \\ &\qquad\left.\frac{K_{mn}\sin\alpha+N(m,n)\cos\alpha}{2\pi}\right). \end{aligned} \tag{29}$$

For our physical problem given in (3) the nomenclature is: $\tilde{D}(\Delta k)=F(u)$ and the available phase-matching values are $\Delta k_{mn}=K_{mn}$ with Fourier coefficients ρ_{mn}.

REFERENCES

[1] R. Lifshitz, A. Arie, and A. Bahabad, "Photonic quasi-crystals for nonlinear optical frequency conversion," *Phys. Rev. Lett.*, vol. 95, no. 13, p. 13901, Sep. 2005.

[2] J. A. Armstrong, N. Bloembergen, J. Ducuing, and P. S. Pershan, "Interactions between light waves in a nonlinear dielectric," *Phys. Rev.*, vol. 127, pp. 1918–1939, Sep. 1962.

[3] M. M. Fejer, G. A. Magel, D. H. Jundt, and R. L. Byer, "Quasi-phase-matched second harmonic generation—Tuning and tolerances," *IEEE J. Quantum Electron.*, vol. 28, no. 11, pp. 2631–2654, Nov. 1992.

[4] V. Berger, "Nonlinear photonic crystals," *Phys. Rev. Lett.*, vol. 81, no. 19, pp. 4136–4139, Nov. 1998.

[5] N. G. R. Broderick, G. W. Ross, H. L. Offerhaus, D. J. Richardson, and D. C. Hanna, "Hexagonally poled lithium niobate: A 2-D nonlinear photonic crystal," *Phys. Rev. Lett.*, vol. 84, no. 19, pp. 4345–4348, May 2000.

[6] S. M. Russell, P. E. Powers, M. J. Missey, and K. L. Schepler, "Broadband midinfrared generation with 2-D quasi-phase-matched structures," *IEEE J. Quantum Electron.*, vol. 37, no. 7, pp. 877–887, Jul. 2001.

[7] A. Arie, N. Habshoosh, and A. Bahabad, "Quasi phase-matching in 2-D nonlinear photonic crystals," *Opt. Quantum Electron.*, vol. 39, pp. 361–375, 2007.

[8] A. Chowdhury, C. Staus, B. F. Boland, T. F. Kuech, and L. McCaughan, "Experimental demonstration of 1535 155-nm simultaneous optical wavelength interchange with a nonlinear photonic crystal," *Opt. Lett.*, vol. 26, pp. 1353–1355, 2001.

[9] A. Bahabad, N. Voloch, A. Arie, A. Bruner, and D. Eger, "Unveiling quasi-periodicity through nonlinear wave mixing in periodic media," *Phys. Rev. Lett.*, vol. 98, no. 20, p. 20501, May 2007.

[10] A. Chowdhury, S. C. Hagness, and L. McCaughan, "Simultaneous optical wavelength interchange with a 2-D second-order nonlinear photonic crystal," *Opt. Lett.*, vol. 25, pp. 832–834, Jun. 2000.

[11] R. K. P. Zia and W. J. Dallas, "A simple derivation of quasi-crystalline spectra," *J. Phys. a Math. Gen.*, vol. 18, pp. L341–L345, May 1985.

[12] C. Giacovazzo, H. L. Monaco, G. Artioli, D. Viterbo, G. Ferraris, G. Gilli, G. Zanotti, and M. Catti, *Fundamentals of Crytallography*, 2nd ed. Oxford, U.K.: Oxford Univ. Press, 2002.

[13] C. D. Olds, A. Lax, and G. Davidoff, *The Geometry of Numbers*. Washington, D.C.: The Mathematical Association of America, 2000.

[14] R. Lifshitz, "The square Fibonacci tiling," *J. Alloys Compounds*, vol. 342, pp. 186–190, 2002.

Alon Bahabad received the B.Sc. degree from the Israel Institute of Technology (Technion), Haifa, Isreal, in 1996, and the M.Sc. and Ph.D. degrees from Tel-Aviv University, Tel-Aviv, Israel, in 2003 and 2007, respectively, all in electrical engineering.

Since January 2008, he is a Fulbright Postdoctoral Scholar with JILA, University of Colorado at Boulder, and National Institute of Standards and Technology.

Noa Voloch received the B.Sc. degree from the Israel Institute of Technology (Technion), Haifa, Isreal, in 2004 and the M.Sc. degree from Tel-Aviv University, Tel-Aviv, Israel, in 2007, both in physics. She is currently pursuing her Ph.D. degree in electrical engineering at Tel-Aviv University.

Ady Arie (M'96–SM'99) received the B.Sc. degree in mathematics and physics from the Hebrew University of Jerusalem, Israel, in 1983 and the M.Sc. degree in physics and Ph.D. degree in engineering from Tel-Aviv University, Tel-Aviv, Israel, in 1986 and 1992, respectively.

Between 1991 and 1993, he was a Wolfson and Fulbright Postdoctoral Scholar in the group of Prof. Robert L. Byer at Ginzton Laboratory, Stanford University, Stanford, CA. In 1993 he joined the Department of Physical Electronics, School of Electrical Engineering in the Faculty of Engineering, Tel-Aviv University. Since 2006, he is a Professor of electrical engineering. His research in the last years is in the areas of nonlinear optics and high resolution spectroscopy.

Prof. Arie is a Chair of the Israel Section of IEEE-LEOS, Vice President of the Israeli Lasers and Electro-Optic Society, and a Member of the Optical Society of America.